LANGMUIR

Article

pubs.acs.org/Langmuir

Dual-Responsive Lipid Nanotubes: Two-Way Morphology Control by pH and Redox Effects

Hande Unsal,[†] Judith Schmidt,[§] Yeshayahu Talmon,[§] Leyla Tatar Yildirim,[‡] and Nihal Aydogan*[,†]

[†]Chemical Engineering Department and [‡]Physics Engineering Department, Hacettepe University, Beytepe, 06800 Ankara, Turkey

[§]Department of Chemical Engineering, Technion-Israel Institute of Technology, Haifa 3200003, Israel

Supporting Information

ABSTRACT: Lipid nanotubes are the preferred structures for many applications, especially biological ones, and thus have attracted much interest recently. However, there is still a significant need for developing more lipid nanotubes that are reversibly controllable to improve their functionality and usability. Here, we presented a two-way reversible morphology control of the nanotubes formed by the recently designed molecule AQUA ($C_{25}H_{29}NO_4$). Because of its special design, the AQUA has both pH-sensitive and redox-active characters provided by the carboxylic acid and anthraquinone groups. Upon chemical reduction, the nanotubes turned into thinner ribbons, and this structural transformation was significantly reversible. The reduction of the AQUA nanotubes also switched the nanotubes from electrically conductive to insulative. Nanotube morphology can additionally be altered by decreasing the pH below the pK_a value of the AQUA, at ∼4.9. Decreasing the pH caused the gradual unfolding of the nanotubes, and the interlayer distance in the nanotube's walls increased. This morphological change was fast and reversible at a wide pH range, including the physiological pH. Thus, the molecular design of the AQUA allowed for an unprecedented two-way and reversible morphology control with both redox and pH effects. These unique features make AQUA a very promising candidate for many applications, ranging from electronics to controlled drug delivery.

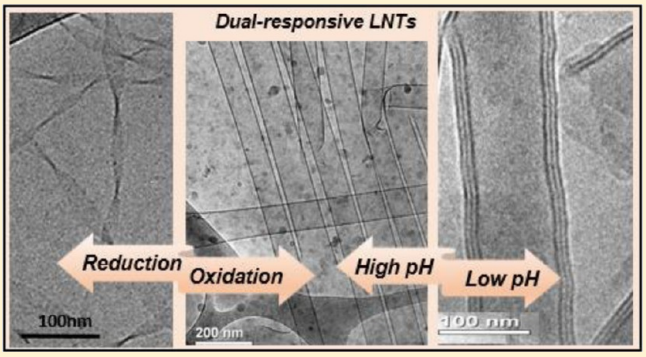

INTRODUCTION

Supramolecular self-assemblies are most remarkable systems for the applications, ranging from biotechnology to electronics.[1−3] Among those nanostructures, lipid nanotubes have significantly more advantages. First, they are highly biocompatible, which is a key property for biotechnological applications. Additionally, both the inner and outer hydrophilic surfaces, identical or different, can be easily functionalized, and it is possible to control the diameters, lengths, and wall thicknesses at a wide range, giving greater control over desired applications established by changing the formation, conditions, and procedures.[4−7] These lipid nanotube specifications make them effective materials in different areas, such as encapsulation,[8] nanochannels,[9] drug delivery,[10,11] templates,[10] nanosensors,[12] electronics,[13] etc. An important goal is to find systems that combine stimuli-response and on-demand reversible control, with all of the above-mentioned lipid nanotube advantages. Directing the assembly and disassembly of the supramolecular aggregates by external stimuli would obviously cause a leap forward in the functionality of the nanotubes.

Triggers that can be used for the stimuli-responsiveness of organic self-assemblies can be physical (mechanical, electric, magnetic, light, and temperature) or chemical (electrochemical, pH, ionic strength, and biochemical).[14] Although self-assembled systems, such as micelles,[15,16] vesicles,[17] monolayers,[18] liquid crystals, etc.,[19] have been studied for a long time, interest in the stimuli-responsiveness and reversible control aspects has been accelerated recently in the field of lipid nanotubes. The studies of stimuli responsive lipid nanotubes are mainly concerned with the control of nanotube morphology by the effects of pH,[20−22] temperature,[23,24] and light.[25,26] In those studies, focusing the light-triggered morphology control, mainly azobenzene, has been used as the functional group responsible for the stimuli-responsive behavior. Moreover, nanotube morphology could be altered by UV irradiation, but those systems lacked the reversibility of this morphological alteration.[25,26] The other trigger widely used for the control of nanotube properties is the solution pH. Many studies show that nanotube formation is affected by the solution pH. However, fewer studies report nanotube structure alteration by changing the solution pH after the formation, and even much fewer studies report reversible morphological alteration by pH. Galantini et al. stated that for the 3b-(2-naphthylamine)-7a,12a-dihydroxycholanic acid molecule the nanotube-to-ribbon transformation is observed reversibly by changing the

Received: January 29, 2016
Revised: May 2, 2016
Published: May 5, 2016

DOI: 10.1021/acs.langmuir.6b00350
Langmuir 2016, 32, 5324−5332

pH from 8.5 to 12, which is a narrow range and above the physiological pH. Thus, that system does not seem to be very useful for biological applications.[20] In the case of glycylglycine bolaamphiphile tubules, the reversible transformation from tubules to helical ribbons occurs when the pH is increased from 4 to 8, but it takes 1 day, and even 10-fold longer time is needed to form ribbons from the tubules.[22] Since the existing systems cannot fulfill the needs for a fast reversible response in a wide pH range, more studies are needed about pH-triggered reversible morphology control to obtain useful systems. Additionally, the variety of triggers used for lipid nanotube morphology control until now has been restricted, and new and useful triggers need to be investigated. Redox-active groups can be used for reversibly controlling conformational changes within a molecule or manipulating the electrical, aggregation, interfacial, and surface properties of materials.[27] For example, by using ferrocene as the redox-active group, reversible control of the aggregate formation or interactions in biological systems can be achieved.[28−32] Anthraquinone is another commonly used redox-active group, which can be reduced and oxidized, both chemically and electrochemically.[33−35] Except for its redox activity, the anthraquinone group also has characteristic self-assembling and charge transport properties. These features lead to applications such as molecular electronics[34,36] and photovoltaics.[37] Although various redox-active systems have been extensively reported in the literature, including one in which the electrical conductivity of self-assembled nanotubes was switched on and off by reduction and reoxidation,[38] reversibly controlling lipid nanotube properties by a redox effect has not been reported.

By considering all of the above-mentioned aspects, here we describe the reversible control of the self-assembled lipid nanotubes formed from the specially designed AQUA ($AQNH(CH_2)_{10}COOH$, where AQ is anthraquinone) molecule (Figure 1a) using different triggers.

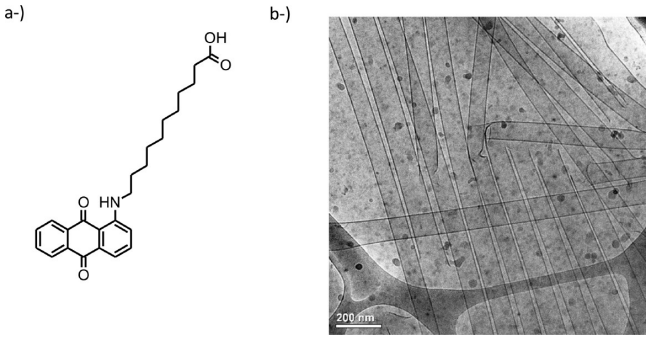

Figure 1. (a) Molecular structure of AQUA. (b) Self-assembled lipid nanotubes of AQUA in an aqueous medium (with equimolar amount of ethanolamine addition, pH 9).

AQUA forms self-assembled lipid nanotubes in water in the presence of equimolar amount of ethanolamine (at the AQUA concentration of 1 wt %) (Figure 1b).[39] The AQUA molecule contains two functional groups: redox-active aminoanthraquinone and pH-sensitive carboxylic acid group, which are linked by an alkyl chain. This rational molecular design gives a dual stimuli-responsive character to AQUA. The dual sensitivity of AQUA is an exceptional feature when compared with the structures found in the literature and provides the possibility of controlling nanotube properties and reversible unfolding/refolding operations by simply changing the solution pH or the redox state of the molecule. This paper mainly deals with the reversible control of AQUA nanotubes by changing the external stimuli. The study comprises two parts: In the first part, the redox-directed reversible morphology control of the self-assemblies is presented; in the second, the effect of pH on the nanotube morphology and its reversibility are described. The morphological and chemical changes induced by the pH changes and redox reaction are clarified by systematical studies to show AQUA nanotubes' possible functionality for potential applications in material sciences and biosciences, ranging from guest entrapment to controlled release, and from electronics to template-assisted synthesis of functional materials.

To the best of our knowledge, AQUA nanotubes are the first redox-active lipid nanotubes whose morphology can be reversibly controlled by both pH and redox effects.

EXPERIMENTAL SECTION

Materials. 1-Chloroanthraquinone (98%), 11-aminoundecanoic acid (97%), ethanolamine (98%), NaOH (98%), hexane (95%), and chloroform (99%) were purchased from Sigma-Aldrich (Germany); dimethyl sulfoxide (DMSO, ACS grade) was purchased from Merck (Germany). These chemicals were used without further purification.

AQUA was synthesized by the reaction of 1-chloroanthraquinone and 11-aminoundecanoic acid in the presence of NaOH.[39]

Formation and Reversible Morphological Tuning of the Lipid Nanotubes. The optimum nanotube formation conditions (i.e., concentration, base type, procedure, etc.) have been determined previously.[39] Briefly, lipid nanotubes were formed by heating aqueous 1 wt % AQUA and an equimolar ethanolamine mixture at 120 °C for 10 min and then cooling the homogeneous hot mixture to room temperature. Ethanolamine is used and found to be the most effective counterion to gain enough water solubility to AQUA molecule which is water insoluble at neutral pH. After the formation of lipid nanotubes at a pH of ∼9, the effects of pH and redox reactions on the nanotube morphology were investigated. For all of the investigations, 1 wt % AQUA aqueous nanotube solution was used as a starting solution, unless otherwise stated. Appropriate amounts of diluted HCl solution were added to the nanotube solution (at pH 9) to induce the pH-triggered morphological alteration. To determine the reversibility of the morphological change, diluted NaOH solution was added to the solutions, until a pH of 9 was re-established. Chemical reduction of the AQUA molecule was carried out by treating the nanotube solution with 10 equimoles of $NaBH_4$ under a nitrogen atmosphere. The completion of the reduction reaction was monitored using Fourier transform infrared (FT-IR) and ultraviolet−visible (UV−vis) spectroscopy. Measurements were performed 2 h after the treatment with $NaBH_4$ to complete the chemical reduction and morphological changes. The effect of a $NaBH_4$ addition on solution pH was also checked. To prove the reversible effect of redox reaction on the morphology of self-assembled structures, the chemically reduced samples were reoxidized by exposure to air for 2−120 h.

Morphological Characterization. Vitrified cryogenic-temperature transmission electron microscopy (cryo-TEM) specimens were prepared in a controlled environment vitrification system at 25 °C and 100% relative humidity. About 3 μL of the sample was placed on a perforated carbon film coating a TEM copper grid and blotted with filter paper. The grid was plunged into liquid ethane at its freezing point. The vitrified specimens were transferred to a 626 Gatan cryo-holder and imaged in an FEI Tecnai T12 G^2 transmission electron microscope at about −175 °C, at a 120 kV acceleration voltage, using low-dose imaging to minimize the electron-beam radiation damage. Images were digitally recorded by a Gatan US1000 high-resolution CCD camera.

FT-IR, X-ray Powder Diffraction, and Electrical Conductivity Analysis. FT-IR (Thermo Scientific Nicolet 6700 FT-IR spectrometer) analyses of the samples, which were dried on glass substrate in a nitrogen atmosphere, were performed using the attenuated total reflection method. X-ray powder diffraction (XRD) measurements

DOI: 10.1021/acs.langmuir.6b00350
Langmuir 2016, 32, 5324−5332

were carried out using a Rigaku D/MAX-2200 diffractometer at 40 kV and 36 mA, with a Cu Kα (λ = 1.5406 Å) radiation source. The specimen preparation for the XRD was the same as that for the FT-IR analyses. For the electrical conductivity measurements, powder, nanotube, and reduced twisted ribbon samples were completely dried in a vacuum oven for 48 h. These samples were turned into pellets under high pressure using a FT-IR pellet preparation press. Next, the conductivity of these pellets, which were not thicker than 0.3 mm, was determined by a homemade four-probe instrument. Measurements were performed at least 5 times with different samples to check the reproducibility of the measurements. Possible effects of added salt on the conductivity measurements were also investigated by adding 10-fold $NaBH_4$ salt to the AQUA nanotubes during the pellet preparation. Although drying the samples may have caused some changes in the measured values, this is valid for all of the samples, and the results were interpreted in a comparative manner.

RESULTS AND DISCUSSION

Effect of the Redox Reactions. As stated earlier, the AQUA molecule is designed to be a multi-stimuli-responsive molecule by the pH-sensitive carboxylic acid and redox-active anthraquinone groups. Here, we investigated the effects of the reduction and reoxidation of the AQUA molecule on the nanotube morphology. AQ is known to be reduced both chemically and electrochemically, and cyclic voltammetry studies have shown that AQUA molecules, which are involved in the nanotubes, can be reduced and reoxidized reversibly with a reduction potential of ~0.8 V vs Ag/AgCl (Gamry potentiostat, model reference 600, USA) (Figure S1). With the information gained from the electrochemical reduction, due to its appropriate reduction potential, $NaBH_4$ was used as the reducing agent for the chemical reduction.[40]

FT-IR Investigations of Redox Reactions. Reduced and oxidized forms of AQUA nanostructures were investigated by FT-IR to quantify the reduction process (Figure 2). There are several important points that one has to consider. First, the AQUA molecule bears two reducible quinone oxygens, and a fraction of the quinone oxygen near the amine group is already charged due to the resonance effect[39] even before the treatment with $NaBH_4$. The possible states, which AQUA molecules could have before and after reduction, are presented in Figure S2. Second, the reduction potentials and the chemical structures of the reduced anthraquinone groups are affected by the solution pH.[41] The quinone oxygen is expected to be protonated following the reduction, if the medium is acidic. Anthraquinone is reduced to the dianion form and stays at that form in aprotic solvents or in a basic environment.[41,42] Since the reduction of AQUA nanotubes is performed at a pH of ~9.0, it is expected that quinone oxygen becomes and stays negatively charged in the reduced form.

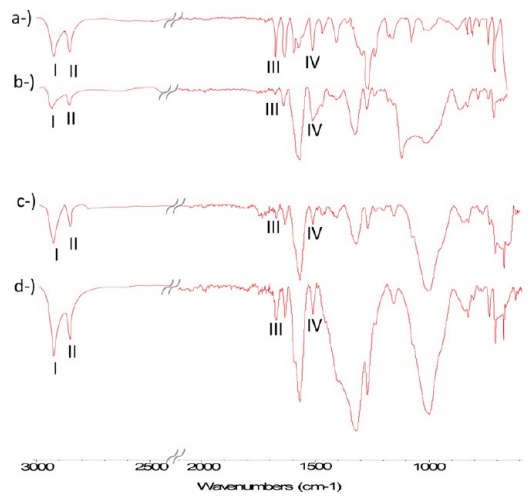

Figure 2. FT-IR spectra of the AQUA: (a) original nanotubes, (b) reduced sample (2 h after treatment with $NaBH_4$), (c) partially reoxidized sample (20 h after exposure to air), and (d) reoxidized sample (90 h after exposure to air). (I) Symmetric and (II) antisymmetric C−H stretching bands; (III) C═O stretching and (IV) $C-O^-$ stretching bands in the anthraquinone group.

The FT-IR spectra of the original AQUA nanotubes and reduced sample are presented in Figures 2a and 2b, respectively. The peak at ~1670 cm^{-1}, which was assigned to the C═O stretching (III) in the anthraquinone group of the unreduced sample,[39] almost disappeared in the reduced sample, since the structure turned to the $C-O^-$, whose peak appeared at ~1500 cm^{-1} (IV). This shows that the reduction of AQUA molecules in the nanotubes was achieved with a considerably high yield. The effect of time and amount of $NaBH_4$ on the reduction efficiency was also investigated, and the optimum conditions were determined as a 2 h incubation time after treatment with 10 times the equivalent of $NaBH_4$ (Table S1).

At 20 h after the reduction the color of the solution reverted to red, and the peak at 1670 cm^{-1} reappeared in the FT-IR spectrum, as given in Figure 2c; this is also valid for Figure 2d, taken 90 h after the reduction. To determine whether the reoxidation of AQUA was complete, the ratios of the peak intensities at 1670 and 1500 cm^{-1} were used for a quantitative evaluation. The I_{1500}/I_{1670} ratio could not be calculated for the reduced sample because the peak at 1670 cm^{-1} was imperceptible, indicating that a very big portion of the quinone oxygen was negatively charged. After 20 h, the I_{1500}/I_{1670} ratio was calculated as 1.36 ± 0.2 and became 0.86 ± 0.1 90 h after exposure to air. This ratio was 0.8 ± 0.1 for the unreduced AQUA nanotubes, meaning that not all, but a significant amount, of the AQUA was reoxidized after 20 h, and the reoxidation was complete after 90 h.

Morphological Characterization. With the addition of a reducing agent into the solution, the solution color turned from opaque red to transparent orange-brown (Figure S3). In addition to the color change, the increased transparency of the reduced solution indicated an aggregate size decrease due to the reduction. When those reduced solutions stayed in contact with the air, the color of the solution turned back to red because of the reoxidation of the AQUA molecule.

Cryo-TEM images of the reduced, partially reoxidized, and reoxidized samples are presented in Figures 3 and 4. Figure 3 shows that the nanotubes seen in Figure 1b are completely transformed into thin ribbons upon reduction, with pitch widths ranging between 12 and 25 nm and pitch lengths of 73−135 nm. The overall lengths of the ribbons were definitely longer than 2 μm. The variation in the ribbon sizes is not huge, but significant. Although the ribbons were not exactly uniform in size, they were quite uniform in shape, and the pitch length/pitch width ratio (L/W) was also constant at 5.5 ± 0.5 for all of the ribbons. This constant ratio has been seen in different systems previously and expressed by scaling laws.[43,44] Helices and nanotubes have cylindrical and mean curvatures, respectively; the curvature of the twisted ribbons is Gaussian-like. The change between these curvature types can be induced by different effects such as temperature, pH, or enantiomeric composition.[45−47] Although the addition of $NaBH_4$ changed the solution pH, this pH fluctuation during the reduction and

DOI: 10.1021/acs.langmuir.6b00350
Langmuir 2016, 32, 5324−5332

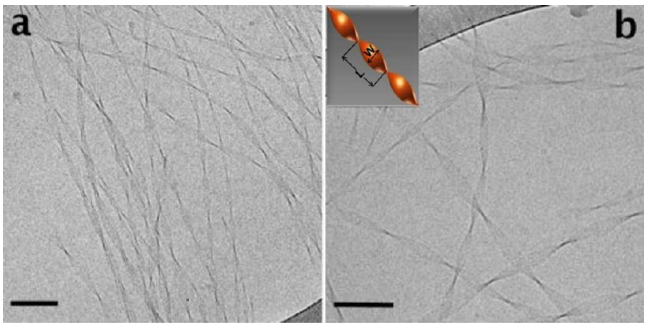

Figure 3. Cryo-TEM images of the reduced AQUA suspensions 2 h after treatment with $NaBH_4$ under nitrogen conditions. The inset in (b) is the schematic presentation of the twisted ribbons; bars = 100 nm.

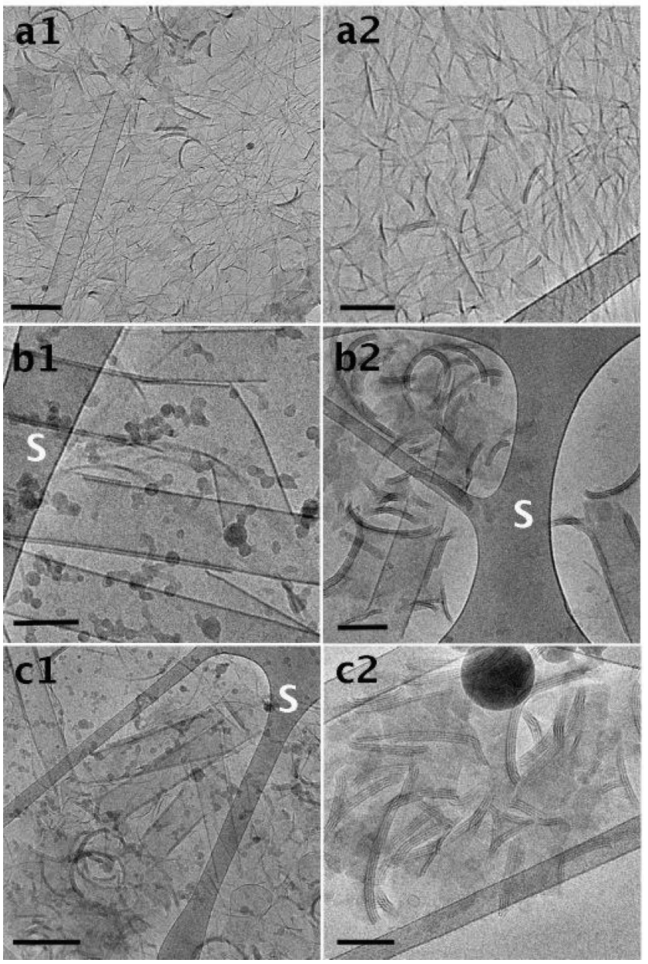

Figure 4. Cryo-TEM images of the AQUA suspensions after reoxidation by air exposure: (a) 20 h (partially reoxidized state); (b) 90 h (reoxidized state); (c) 160 h (reoxidized state). Bars correspond to 100 nm, except for a1 and c1, where they correspond to 200 nm. "S" denotes the carbon support film. Small, dark specs are ice surface contamination. Arrows show multilayered membrane sheets.

reoxidation was quite small (less than 0.5) and did not change the nanotube morphology (Figure S4). In our study, the change from nanotubes to ribbons was driven by the redox effects. Upon reduction, the attraction between the molecules changed, which gave rise to a transformation in the packing of the molecules. It has been reported that when there are strong intermolecular attractions between molecules, tubular-like structures (including helical ribbons) are more favored than twisted ribbons. There have been some examples in which repulsions between molecules have given rise from the transformation of a tubular structure to twisted ribbons.[46] As seen from Figure 2, twisted ribbons formed upon the reduction of the AQUA show that the wavenumbers of symmetric and antisymmetric C−H stretching bands (I and II, respectively) are higher than those of unreduced sample (2919−2930 cm^{-1} for symmetric and 2849−2854 cm^{-1} for antisymmetric bands). The shift to higher wavenumbers is generally proposed to be related with the change in the crystalline structure (toward weakening), which is consistent with our interpretation that the molecular packing of reduced form of AQUA was weak due to the electrostatic repulsion between the anthraquinone groups. Upon exposure to air, the wavenumbers of the C−H stretching bands got closer to those observed in the original tubular form as the reoxidation proceeded, and after 90 h, they turned back to almost their original position for the reoxidized sample. Although the dynamics of this transition are not that clear and need to be investigated further, it is clear that the chemical transformation upon redox reaction is evident and highly reversible.

After the verification of the chemical reversibility of the redox reaction, morphological reversibility investigations were performed. From the cryo-TEM images of the partially reoxidized sample (air exposure), long or short nanotubes, as well as multilayered-membrane sheets, and twisted narrow ribbons are seen (Figure 4a). Although some nanotubes were re-formed, there still existed a significant portion of ribbons. When the exposure time was increased to 90 h, almost all of the twisted ribbons had disappeared, and the number of nanotubes increased, as shown in Figure 4b. Some of those nanotubes were shorter than the original ones. Additionally, sheet-type structures existed in the solution. We believe that the sheet-type structures are intermediates that had not completed their transformation to the smooth nanotubes. Observations of intermediate structures will provide evidence for the formation mechanism and kinetic of processes that lead the formation of large structures like nanotubes. It has been observed previously in numerous studies that the twisted ribbons can transform into tubular structures with a pathway of twisted ribbon → helices→ nanotubes. The transformation from twisted ribbons to helical intermediates occurs at a definite width/thickness ratio as the ribbons continue to aggregate laterally and reach the necessary width for this curvature alteration. The helical intermediates then evolve to nanotubes.[48−50] There could be different possible mechanisms that favor thermodynamically the formation of tubular structures such as Oswald ripening. We believe that in our system, as the reoxidation proceeded, the charge characteristics and solubility of the AQUA molecules changed. That altered the electrostatic interactions between the AQUA−AQUA molecules as well as the interactions between the AQUA−solvent molecules due to the hydrophilicity change, causing this very significant morphological transformation. The net negative charge of the AQUA was higher for the reduced state, so during reoxidation, the twisted ribbons' lateral aggregation tendency might increase with the decreasing electrostatic repulsion, and this lateral aggregation may have induced the curvature transformation that eventually results in the re-formation of nanotube geometry.

DOI: 10.1021/acs.langmuir.6b00350
Langmuir 2016, 32, 5324−5332

FT-IR analysis indicates that although some of the AQUA molecules were reoxidized in 20 h, complete reoxidation takes a longer time.

It was seen from the TEM micrographs that after 90 h the transformation into nanotubes was considerable but still incomplete, and there were some multilayered curved sheets. It is proposed that these intermediate multilayered structures give rise to tubular structures, which are also characterized to have multilayered lamellar structures (see discussion below). This might be one of the reasons why ribbons still existed after 20 h. After 90 h, the transformation into nanotubes was considerable, but in some of the nanotubes, the interlayer spacing in the nanotube wall was higher than that in the original nanotubes. That situation did not change considerably after 160 h (Figure 4c).

Ten times equivalents of $NaBH_4$, with respect to the AQUA, was used to achieve complete reduction, and so, there existed large amounts of salt in the solution during the re-formation of the nanotubes. This might have caused the morphological difference of the re-formed nanotubes since it changes the intermolecular electrostatic interactions. Thus, the effect of salt in the self-assembly behavior of the AQUA has also been investigated. We found that the properties of the nanotubes did not change with a salt concentration of up to 25 mM, but at 100 mM, mostly sheet-type structures were formed (Figure S5). The need for an excess amount of reducing salt obstructed the reversible re-formation of some of the nanotubes, but we have still shown that a considerable amount of nanotubes can be reversibly destroyed and re-formed by the redox reactions.

There are very few reports in the literature of redox-active self-assembled nanotubes, and those studies are concerned primarily with the change in the electrical conductivity of the nanotubes with no reference to the change in the aggregate morphology.[38] To our knowledge, reversible disintegration and re-formation of the lipid nanotube structure by redox reactions is reported here for the first time.

XRD Analysis. To gain additional information about the effect of reduction and reoxidization on the molecular level, and the reversibility of the morphological change, XRD was also performed on the reduced and reoxidized samples to a different extent. The small-angle region could not be reached, which is needed to observe the exact tubular structure by the available SAXS instrument. However, when the results obtained from TEM and cryo-TEM were compared, it was seen that the nanotube properties did not change when dried[39] (Figure S6). Thus, powder XRD was considered as a convenient analysis method for our system.

The XRD peaks of the original AQUA nanotubes, which are labeled A1, A2, A3, and A4, are seen at 2.2°, 4.4°, 6.6°, and 8.8° 2θ values, respectively (Figure 5). These periodical peak locations indicate that the AQUA nanotube wall has a lamellar multilayered structure. When the nanotubes were reduced (at pH 9), the peaks seen in the XRD pattern shifted to higher 2θ values, which were 5.1° and 7.5° for the B1 and B2 peaks, respectively. Since the anthraquinone groups in the reduced AQUA molecules had a net negative charge, the electrostatic repulsion between the molecules increased. In addition to the change of the solvophilicity of the AQUA in water, the increase caused the AQUA molecules to be packed differently, probably less tight. By considering the shift of the *d*-spacings to smaller values, the molecules may become more tilted in the membrane. Moreover, the peak periodicity disappeared after the reduction, indicating that the smooth multilayered structure

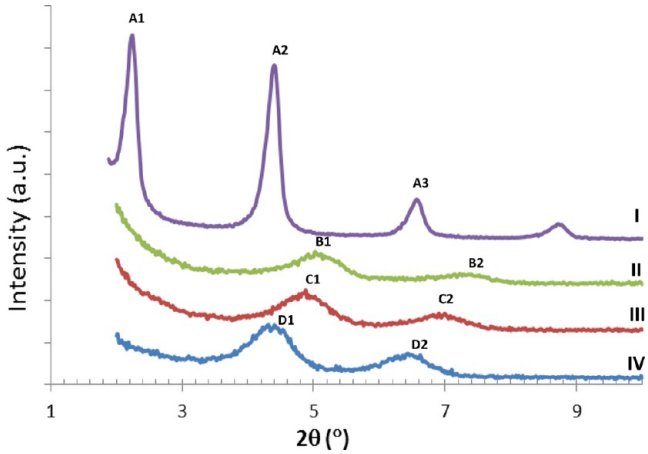

Figure 5. XRD curves of the AQUA nanostructures: (I) original nanotubes; (II) reduced sample (2 h after treatment with $NaBH_4$); (III) partially reoxidized sample (20 h after exposure to air); (IV) reoxidized sample (90 h after exposure to air).

of the membranes was deformed. Thus, the arrangement or orientation of the molecules in the membrane changed upon reduction, and this considerably changed the aggregate morphology. At 20 h after the reduction, when the AQUA molecules were partially reoxidized, a little shift to smaller angles in comparison with the unreduced sample's XRD pattern was observed, and peaks C1 and C2 appeared at 4.9° and 6.9°, respectively. After 90 h, the peak positions of D1 and D2 turned back to 4.4° and 6.6°, respectively. The broader peaks for the reoxidized samples indicate that although the nanotubes were re-formed with the same XRD peak positions, the reoxidized sample was somewhat less ordered than the original nanotube solution.

Electrical Conductivity Measurements. The AQUA molecule has been specially designed to form "smart" nanotubes with multifarious features and applications. The fastidiously selected anthraquinone group in the AQUA molecule has still further contributions to its abilities, such as distinguishing electrical properties, in addition to its aforementioned redox activity and self-assembly properties. It is known that the electrical conductivity is significantly affected by the molecular arrangement and the redox state.[51,52] Hence, conductivity measurements were performed for the powder AQUA (as obtained from the synthesis), AQUA nanotubes, and AQUA twisted ribbons (reduced samples) and determined as 4.3×10^{-5}, 1.19×10^{-3}, and 2.1×10^{-5} S/cm, respectively. The electrical conductivity of some of the anthraquinone derivatives lies between 10^{-6} and 10^{-12} S/cm,[53] and even the powder form of AQUA had a higher conductivity than most of its homologues. AQUA molecules are arranged in a highly ordered helical manner in the nanotube structure, as deduced from the previous polarimeter results and STEM images.[39] This gives rise to an increase at the measured electrical conductivity by nearly 100 times. This result is consistent with the fact that the organization of molecules significantly changes their electrical and optical properties;[54,55] thus, the ordered helical packing of the AQUA nanotubes is believed to be effective in providing significant electrical conductivity. Additionally, the tunability of the charge and morphological characteristics of the AQUA nanotubes provides tunability for the charge transport properties of these structures, and upon chemical reduction of the AQUA nanotubes, the electrical conductivity value was

DOI: 10.1021/acs.langmuir.6b00350
Langmuir 2016, 32, 5324−5332

determined to be at least 2 orders of magnitude less. To confirm that the determined difference in the measured conductivities of the AQUA nanotubes and twisted ribbons was not caused by excess $NaBH_4$ salt in the pellets of the reduced sample, $NaBH_4$ powder was mixed with the AQUA nanotubes in the solid state, without the chemical reduction of the AQUA, and it was seen that the conductivity value did not change significantly. It has been stated previously that the molecular arrangement changes upon reduction, aggregates become smaller, and the smooth layered structure is deformed. Moreover, in a previous study, it was found that the increase in the crystallite size increases the conductivity.[56] Thus, it is thought that both the change in the conjugation of the AQ ring and the transformation of the aggregate morphology have a role in this significant conductivity decrease. This decrease is such that the aggregates switch from significantly conductive to almost insulative.

Another important property for electronic applications is the ordered alignment of the nanotubes to form a regular film on different substrates. It has been found that AQUA nanotubes are spontaneously aligned in a parallel fashion on two different substrates, one of which is Teflon and the other is glass (Figure 6). For many organic and inorganic nanotubes, lots of effort is

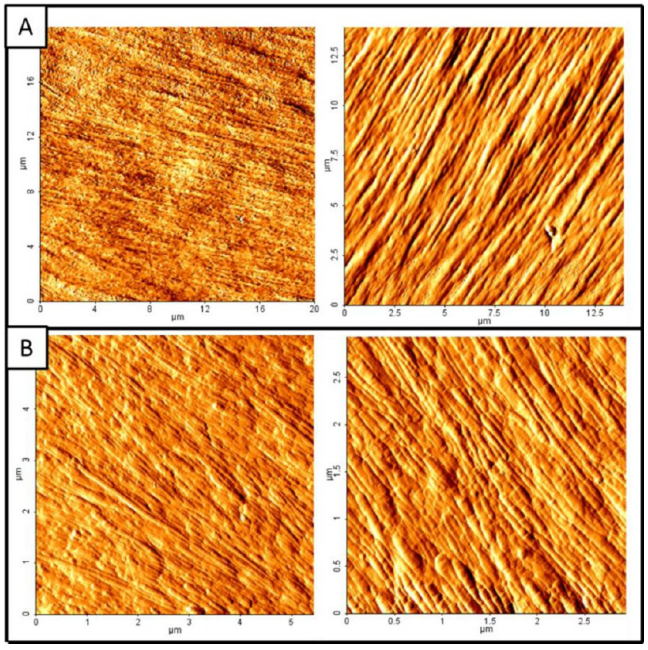

Figure 6. AFM images of the AQUA nanotubes dried on (A) a glass surface and (B) Teflon tape in "error" mode.

spent and different methods are required to obtain an ordered alignment, but AQUA nanotubes are able to arrange as a regular film of parallel nanotubes when just dropped into the substrate surface without needing any extra treatment. This is another important advantage of our structures.

These results show that AQUA nanotubes have adjustable electrical properties ranging in a wide range from conductive to insulative as well as their self-alignment properties. Because of these properties, they have the potential to be used in nanoelectronic devices and they are worth further investigation.

Effect of the Solution pH. The cryo-TEM image in Figure 1b shows that the diameters and lengths of AQUA nanotubes were in the range of 110−190 nm and 4−8 μm, respectively, at pH 9. The AQUA molecule is pH sensitive, owing to the carboxylic acid group, as well as being redox-active. Thus, we studied the nanotube properties at different solution pHs, namely, 7, 5, 4, 3, and 1, after forming the AQUA nanotubes in the aforementioned conditions (pH 9) (see Figure S6).

As seen in Figure 7, at pH 9, smooth nanotubes existed as the only dominant aggregate type in the solution. The wall and

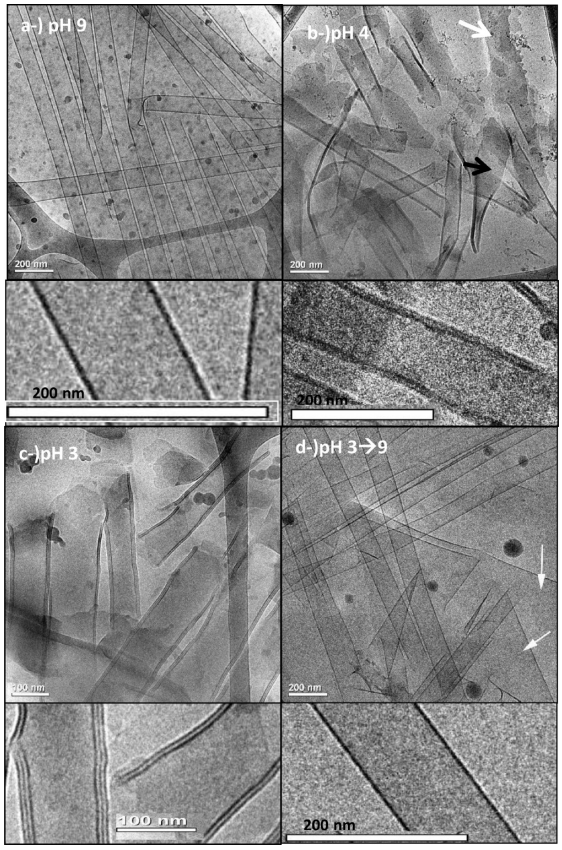

Figure 7. Cryo-TEM images of the AQUA suspensions: (a) at formation conditions (pH 9); (b) at pH 4; (c) at pH 3; (d) at pH 9, prepared from the sample at pH 3 by the addition of NaOH. Black arrow indicates the structurally deformed nanotube; white arrows indicate fully open sheets.

core sides of the nanotubes were evidently discernible. Cryo-TEM gave a wall thickness of 5 ± 1 nm at pH 9. The answer to the question of whether the tubes have multiwalls or single wall was supported with the help of the XRD spectra. However, it was not very clear from the cryo-TEM images of the nanotubes at pH 9 that the AQUA nanotubes have multilayered wall structures in which the separation distance between layers was very small. The nanotube morphology did not show any changes with a lowering of the pH level down to pH 5, and below that point, noticeable changes occurred (see Figure 7). The pK_a of the COOH in the AQUA was calculated as 4.9. At pH values, especially below the pK_a, much of the carboxylic acid groups on the nanotube surfaces became nonionic. This situation acts as a breakpoint for the morphological alteration with the pH effect, indicating that electrostatic effects have a high impact on the AQUA self-assembly. From the UV−vis spectra of the AQUA nanotube solutions at pH 9 and 6, it was seen that the absorbance value decreased at a lower pH (Figure S7). This shows that the intermolecular interactions gradually decreased with a decreasing pH. The intermolecular interaction

DOI: 10.1021/acs.langmuir.6b00350
Langmuir 2016, 32, 5324−5332

was stronger when the AQUA molecules were mostly negatively charged and was weaker at lower pH levels, where the H-bonds between the COOH groups might be more profound, so it is believed that electrostatic interactions had a dominant and promoting effect on the nanotube formation.

When the pH was decreased to 4, the homogeneous and smooth character of the solution disappeared, and the nanostructures shown in Figure 7b appeared. At pH 4, there existed a mixture of fully opened sheets and structurally deformed nanotubes, along with some aggregates preserving their smooth tubular geometry. Smooth nanotubes were no longer the dominant aggregate type at pH 4, and the remaining nanotubes had different morphological properties. The total wall thickness increased from 5 ± 1 to 10 ± 2 nm, as the solution pH decreased from 9 to 4. With a further decrease of the pH to 3, similar results were observed (Figure 7c) as with a pH of 4, but there was a further increase in the total wall thickness, i.e., 11 ± 2 nm at a pH of 3. In Figure 7b, the existence of the multilayered wall structure can be vaguely seen for the sample at a pH of 4, but prominent separation of the layers is clearly observed in the magnified image in Figure 7c at a pH of 3. As mentioned above, the XRD pattern given in Figure 5a shows a lamellar wall structure consisting of stacked layers. Moreover, it was previously stated that AQUA nanotube walls consist of symmetrical monolayers through the agency of the FT-IR and zeta-potential results as well as the TEM and XRD analysis. The absence of lateral carboxylic acid H-bond peaks in the FT-IR spectrum and the lower surface charge density of AQUA nanotubes compared with the nanotubes containing only carboxylate groups on the nanotube walls (which are calculated from zeta potential measurements) shows the symmetrical monolayer structure.[39] Thus, a wall thickness of 5 ± 1 nm was obtained from the cryo-TEM points out existence of 2 or 3 layers in the walls, since the molecular length of the AQUA was calculated as ∼2 nm.[39] Although the nanotubes had a multilayered wall structure at a pH of 9, they are closely packed and individual layers could not be observed in the cryo-TEM images. However, as the pH decreased, the individual layers became observable. These results show that the pH decrease caused the gradual unfolding of the tube structure and the distance between the layers in the wall structure increased. A further decrease of the pH to 1 led to the complete unfolding of the nanotubes into sheet-like structures. The morphology of the AQUA self-assembles at higher pH levels was also investigated (Figure S4). It was seen that at pH levels higher than 9 the AQUA nanotubes retained their tubular structure.

To test the reversibility of the pH effect, we imaged samples whose pH level was readjusted to 9 from 3 (Figure 7d). They exhibited nanotubes of similar morphological and dimensional properties to the stock solution (at pH 9), along with some flat sheets, and shorter, sometimes imperfect, tubes. There was no evidence that the nanotubes with the higher interlayer spacing at a pH of 3 remain; thus, it was concluded that the structures that had slightly unfolded, but had not totally lost their tubular geometry, did regain their original properties. However, at least some of the nanotubes that had been fully unfolded into sheets could not be folded reversibly into nanotubes again. When the pH level was increased back to 9 from 1, the pH-dependent morphology change became mostly irreversible (Figure S8), although the AQUA molecule was chemically stable at this lower pH, as indicated by the FT-IR measurements (Figure S9). By taking these findings into consideration, it is understood that the irreversibility of the morphological change at a pH of 1 is the result of the fact that most of the nanotubes had turned into flat sheets at that pH.

To summarize, reversibly tuning of the nanotube morphology was achieved to a large extent with a wide pH range of 3 to 9. In previous studies, only the effect of the pH under nanotube formation conditions was investigated; there are fewer studies of the transformation of the tubular structure by pH change after formation. Among these studies dealing with the reversibility of the nanotube morphology control by a change in the pH, there have been no examples whose morphology can be reversibly tuned with such a wide pH range and fast response (less than 30 min). Either the pH range for reversible control was between 8.5 and 12, or changing the morphology, and then returning to the original state, took 11 days in previous studies.[22] Obviously, the AQUA outscores them by having a fast reversible morphology change with a wide pH range, and has a much higher potential for various application areas.

The morphological changes by solution pH are caused by the changes in the charge characteristics of the AQUA; the equilibrium composition of the resonance state might be affected by the solution pH,[39,57,58] along with the existence of a carboxylic acid to carboxylate transformation. One might find it interesting that the spacing between the layers increases with the decreasing pH, where the net negative charge is lower. However, it is believed that there exists an attraction between the negatively charged carboxylate groups and the partially positively charged part of the aminoanthraquinone group (resonance effect), which stabilizes the multilayer wall structure of the nanotubes at higher pH values. From Table S1 and Figure S9 it is concluded that at all of the investigated pH values the resonance state is valid and in agreement with the literature, and the equilibrium conversion is a little higher for higher pH values (see Figure S2).[57]

XRD was performed to obtain more insight into the effect of pH on the molecular level. The uniformly distributed peaks in the XRD spectrum, as mentioned above, indicate a smooth layered structure in the nanotubes;[59] for the samples at different pH values, below or above the pK_a of AQUA (Figure 8 and Figure S10), the peak positions do not change although significant changes are seen in the cryo-TEM images. This suggests that the molecular arrangement in the monolayer does not change significantly, but gradual unfolding occurs with pH decrease causing increased separation of the monolayers.

■ CONCLUSIONS

The smart nanotubes formed by AQUA molecule have a dual stimuli-responsive character; morphological alterations can be triggered by either pH or redox effects. Upon chemical reduction, AQUA nanotubes are transformed into thin ribbons, which are totally uniform in shape and have a constant pitch length/pitch width value. The morphological change with the redox effect is considerably reversible, with the disappearance of the ribbons and re-formation of a significant amount of smooth nanotubes upon reoxidation. AQUA nanotubes have characteristic electrical properties, which can be turned from lower conductivity values to a considerably conductive state by the effect of chemical reduction. Furthermore, the reversibility of the change with the redox effect as well as the self-alignment characteristic makes the AQUA nanotubes highly functional candidates for electronics applications. Additionally, the nanotube morphology suddenly disrupts as the pH level is

DOI: 10.1021/acs.langmuir.6b00350
Langmuir 2016, 32, 5324−5332

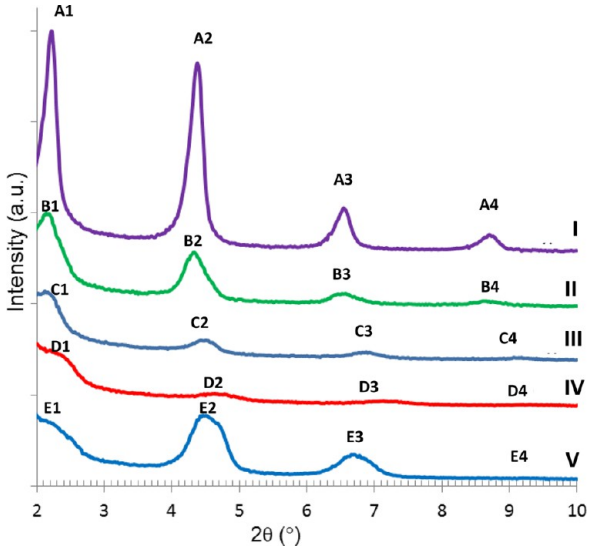

Figure 8. XRD curves of the AQUA nanotubes at (I) pH 9, (II) pH 7, (III) pH 5, (IV) pH 3, and (V) pH 9 (prepared by adding NaOH solution to nanotube solution at pH 3).

decreased below the pK_a value of the AQUA at pH 4.9. The pH-triggered morphological change is also reversible in a uniquely wide pH range (i.e., between pH 3 and 12) among pH-sensitive nanotubes and with a very fast response. Thus, through the rational molecular design of the AQUA, self-assembled redox active nanotubes, whose morphology can be reversibly controlled in a two-way fashion and whose electrical properties can also be tuned, are obtained. Because of these outstanding features, AQUA nanotubes should have many applications with biological and electronic aspects.

■ ASSOCIATED CONTENT

Supporting Information

The Supporting Information is available free of charge on the ACS Publications website at DOI: 10.1021/acs.langmuir.6b00350.

XRD and FT-IR spectra, AFM, and TEM images of the solutions at different pH levels, and at different electrolyte concentrations, as well as the CV of the AQUA nanotube solution (PDF)

■ AUTHOR INFORMATION

Corresponding Author

*Fax +90 312 2992124, e-mail anihal@hacettepe.edu.tr (N.A.).

Notes

The authors declare no competing financial interest.

■ ACKNOWLEDGMENTS

This work was supported by the Scientific and Technical Research Council of Turkey (TÜBİTAK) through Grant 111M143. The cryo-TEM work was performed at The Laboratory for Electron Microscopy of Soft Matter, supported by the Technion Russell Berrie Nanotechnology Institute (RBNI). We express our thanks to Prof. Dr. Kadir Pekmez for his helpful discussions during the conductivity investigation.

■ REFERENCES

(1) Nie, Z.; Petukhova, A.; Kumacheva, E. Properties and emerging applications of self-assembled structures made from inorganic nanoparticles. *Nat. Nanotechnol.* **2010**, *5*, 15−25.

(2) Pignatello, R. *Biomaterials Science and Engineering*; InTech: Croatia, 2011; Chapter 5, pp 115−138.

(3) Lee, J. H.; Choi, Y. J.; Lim, Y. B. Self-assembled filamentous nanostructures for drug/gene delivery applications. *Expert Opin. Drug Delivery* **2010**, *7*, 341−351.

(4) Shimizu, T.; Masuda, M.; Minamikawa, H. Supramolecular nanotube architectures based on amphiphilic molecules. *Chem. Rev.* **2005**, *105*, 1401−1444.

(5) Zhu, C.; Zhang, Y.; Wang, Y.; Li, Q.; Mu, W.; Han, X. Point-to-Plane nonhomogeneous electric-field-induced simultaneous formation of giant unilamellar vesicles (guvs) and lipid tubes. *Chem. - Eur. J.* **2016**, *22*, 2906−2909.

(6) Wang, Y.; Ma, S.; Su, Y.; Han, X. Palladium nanotubes formed by lipid tubule templating and their application in ethanol electrocatalysis. *Chem. - Eur. J.* **2015**, *21*, 6084−6089.

(7) Bi, H.; Fu, D.; Wang, L.; Han, X. Lipid nanotube formation using space-regulated electric field above interdigitated electrodes. *ACS Nano* **2014**, *8*, 3961−3969.

(8) Shimizu, T. Self-assembled lipid nanotube hosts: The dimension control for encapsulation of nanometer-scale guest substances. *J. Polym. Sci., Part A: Polym. Chem.* **2006**, *44*, 5137−5152.

(9) Hurtig, J.; Orwar, O. Injection and transport of bacteria in nanotube−vesicle networks. *Soft Matter* **2008**, *4*, 1515−1520.

(10) Zhou, Y. Lipid nanotubes: Formation, templating nano-structuresand drug nanocarriers. *Crit. Rev. Solid State Mater. Sci.* **2008**, *33*, 183−196.

(11) Kameta, N.; Minamikawa, H.; Masuda, M.; Mizuno, G.; Shimizu, T. Controllable biomolecule release from self-assembled organic nanotubes with asymmetric surfaces: pH and temperature dependence. *Soft Matter* **2008**, *4*, 1681−1687.

(12) US Patent 7 745 856, 2010.

(13) Liu, R.; Cho, S.; Lee, S. B. Poly(3,4-ethylenedioxythiophene) nanotubes as electrode materials for a high-powered supercapacitor. *Nanotechnology* **2008**, *19*, 215710.

(14) Liu, F.; Urban, M. W. Recent advances and challenges in designing stimuli-responsive polymers. *Prog. Polym. Sci.* **2010**, *35*, 3−23.

(15) Lee, H. I.; Wu, W.; Oh, J. K.; Mueller, L.; Sherwood, G.; Peteanu, L.; Kowalewski, T.; Matyjaszewski, K. Light-induced reversible formation of polymeric micelles. *Angew. Chem., Int. Ed.* **2007**, *46*, 2453−2457.

(16) LaRue, I.; Adam, M.; Pitsikalis, M.; Hadjichristidis, N.; Rubinstein, M.; Sheiko, S. S. Reversible morphological transitions of polystyrene-b-polyisoprene micelles. *Macromolecules* **2006**, *39*, 309−314.

(17) Xing, L. B.; Yu, S.; Wang, X. J.; Wang, G. X.; Chen, B.; Zhang, L. P.; Tung, C. H.; Wu, L. Z. Reversible multistimuli-responsive vesicles formed by an amphiphilic cationic platinum(II) terpyridyl complex with a ferrocene unit in water. *Chem. Commun.* **2012**, *48*, 10886−10888.

(18) Nandivada, H.; Ross, A. M.; Lahann, J. Stimuli-responsive monolayers for biotechnology. *Prog. Polym. Sci.* **2010**, *35*, 141−154.

(19) Agrawal, A.; Luchette, P.; Palffy-Muhoray, P.; Biswal, S. L.; Chapman, W. G.; Verduzco, R. Surface wrinkling in liquid crystal elastomers. *Soft Matter* **2012**, *8*, 7138−7142.

(20) Chiara di Gregorio, M.; Pavel, N. V.; Jover, A.; Meijide, F.; Tato, J. V.; Tellini, V. H. S.; Vargas, A. A.; Regev, O.; Kasavi, Y.; Schille'n, K.; Galantini, L. pH sensitive tubules of a bile acid derivative:A tubule opening by release of wall leaves. *Phys. Chem. Chem. Phys.* **2013**, *15*, 7560−7566.

(21) di Gregorio, M. C.; Varenik, M.; Gubitosi, M.; Travaglini, L.; Pavel, N. V.; Jover, A.; Meijide, F.; Regev, O.; Galantini, L. Multi stimuli response of a single surfactant presenting a rich self-assembly behavior. *RSC Adv.* **2015**, *5*, 37800−37806.

DOI: 10.1021/acs.langmuir.6b00350
Langmuir 2016, 32, 5324−5332

(22) Matsui, H.; Gologan, B. Crystalline glycylglycine bolaamphiphile tubules and their pH-sensitive structural transformation. *J. Phys. Chem. B* **2000**, *104*, 3383−3386.
(23) Kawano, S.; Urban, M. W. Expandable temperature-responsive polymeric nanotubes. *ACS Macro Lett.* **2012**, *1*, 232−235.
(24) Douliez, J. P.; Pontoire, B.; Gaillard, C. Lipid tubes with a temperature-tunable diameter. *ChemPhysChem* **2006**, *7*, 2071−2073.
(25) Hu, Q.; Wang, Y.; Jia, J.; Wang, C.; Feng, L.; Dong, R.; Sun, X.; Hao, J. Photoresponsive chiral nanotubes of achiral amphiphilic azobenzene. *Soft Matter* **2012**, *8*, 11492−11498.
(26) Kameta, N.; Tanaka, A.; Akiyama, H.; Minamikawa, H.; Masuda, M.; T. Shimizu, T. Photoresponsive soft nanotubes for controlled guest release. *Chem. - Eur. J.* **2011**, *17*, 5251−5255.
(27) Nijhuis, C. A.; Ravoo, B. J.; Huskens, J.; Reinhoudt, D. N. Electrochemically controlled supramolecular systems. *Coord. Chem. Rev.* **2007**, *251*, 1761−1780.
(28) Aytar, B. S.; Muller, J. P. E.; Golan, S.; Kondo, Y.; Talmon, Y.; Abbott, N. L.; Lynn, D. M. Chemical oxidation of a redox-active, ferrocene-containing cationic lipid: Influence on interactions with dna and characterization in the context of cell transfection. *J. Colloid Interface Sci.* **2012**, *387*, 56−64.
(29) Aydogan, N.; Aldis, N. Tuning surface tension and aggregate shape via a novel redox active fluorocarbon-hydrocarbon hybrid surfactant. *Langmuir* **2006**, *22*, 2028−2033.
(30) Kakizawa, Y.; Sakai, H.; Yamaguchi, A.; Kondo, Y.; Yoshino, N.; Abe, M. Electrochemical control of vesicle formation with a double-tailed cationic surfactant bearing ferrocenyl moieties. *Langmuir* **2001**, *17*, 8044−8048.
(31) Anton, P.; Heinze, J.; Laschewsky, A. Redox-active monomeric and polymeric surfactants. *Langmuir* **1993**, *9*, 77−85.
(32) Aydogan, N.; Abbott, N. L. Comparison of the surface activity and bulk aggregation of ferrocenyl surfactants with cationic and anionic headgroups. *Langmuir* **2001**, *17*, 5703−5706.
(33) Susan, M. A. B. H.; Tani, K.; Watanabe, M. Surface activity and redox behavior of nonionic surfactants containing an anthraquinone group as the redox-active site. *Colloid Polym. Sci.* **1999**, *277*, 1125−1133.
(34) Murschell, A. E.; Sutherland, T. C. Anthraquinone-based discotic liquid crystals. *Langmuir* **2010**, *26*, 12859−12866.
(35) Abel, E.; Castro, R.; McRobbie, I. M.; Barbour, L.; Atwood, J. L.; Kaifer, A. E.; Gokel, G. W. A redox-switchable molecular receptor based on anthraquinone. *Supramol. Chem.* **1998**, *9*, 199−202.
(36) van Dijk, E. H.; Myles, D. J. T.; van der Veen, M. H.; Hummelen, J. C. Synthesis and properties of an anthraquinone-based redox switch for molecular electronics. *Org. Lett.* **2006**, *8*, 2333−2336.
(37) Murschell, A. E.; Kan, W. H.; Thangadurai, V.; Sutherland, T. C. Anthraquinone derivatives as electron-acceptors with liquid crystalline properties. *Phys. Chem. Chem. Phys.* **2012**, *14*, 4626−4634.
(38) Hill, J. P.; Jin, W.; Kosaka, A.; Fukushima, T.; Ichihara, H.; Shimomura, T.; Ito, K.; Hashizume, T.; Ishii, V.; Aida, T. Self-assembled hexa-peri-hexabenzocoronene graphitic nanotube. *Science* **2004**, *304*, 1481−1483.
(39) Unsal, H.; Aydogan, N. Formation of chiral nanotubes by the novel anthraquinone containing-achiral molecule. *J. Colloid Interface Sci.* **2013**, *394*, 301−311.
(40) Kumar, A.; Saxena, A.; De, A.; Shankar, R.; Mozumdar, S. Facile synthesis of size-tunable copper and copper oxide nanoparticles using reverse microemulsions. *RSC Adv.* **2013**, *3*, 5015−5021.
(41) Susan, A. B. H.; Begum, M.; Takeoka, Y.; Watanabe, M. Effect of pH and the extent of micellization on the redox behavior of non-ionic surfactants containing an anthraquinone group. *J. Electroanal. Chem.* **2000**, *481*, 192−199.
(42) Shamsipur, M.; Salimi, A.; Golabi, S. M.; Sharghi, H.; Mousavi, M. F. Electrochemical properties of modified carbon paste electrodes containing some amino derivatives of 9, 10-anthraquinone. *J. Solid State Electrochem.* **2001**, *5*, 68−73.
(43) Adamcik, J.; Jung, J.-M.; Flakowski, J.; De Los Rios, P.; Dietler, G.; Mezzenga, R. Understanding amyloid aggregation by statistical analysis of atomic force microscopy images. *Nat. Nanotechnol.* **2010**, *5*, 423−428.
(44) Lara, C.; Adamcik, J.; Jordens, S.; Mezzenga, R. General self-assembly mechanism converting hydrolyzed globular proteins into giant multistranded amyloid ribbons. *Biomacromolecules* **2011**, *12*, 1868−1875.
(45) Hamley, I. W.; Dehsorkhi, A.; Castelletto, V.; Furzeland, S.; Atkins, D.; Seitsonen, J.; Ruokolainen, J. Reversible helical unwinding transition of a self-assembling peptide amphiphile. *Soft Matter* **2013**, *9*, 9290−9293.
(46) Uesaka, A.; Ueda, M.; Makino, A.; Imai, T.; Sugiyama, J.; Kimura, S. Morphology control between twisted ribbon, helical ribbon, and nanotube self-assemblies with his-containing helical peptides in response to pH change. *Langmuir* **2014**, *30*, 1022−1028.
(47) Oda, R.; Huc, I.; Schmutz, M.; Candau, S. J.; MacKintosh, F. C. Tuning bilayer twist using chiral counterions. *Nature* **1999**, *399*, 566−569.
(48) Adamcik, J.; Castelletto, V.; Bolisetty, S.; Hamley, I. W.; Mezzenga, R. Direct observation of time-resolved polymorphic states in the self-assembly of end-capped heptapeptides. *Angew. Chem., Int. Ed.* **2011**, *50*, 5495−5498.
(49) Ziserman, L.; Lee, H.-Y.; Raghavan, S. R.; Mor, A.; Danino, D. Unraveling the mechanism of nanotube formation by chiral self-assembly of amphiphiles. *J. Am. Chem. Soc.* **2011**, *133*, 2511−2517.
(50) Pashuck, E. T.; Stupp, S. I. Direct observation of morphological transformation from twisted ribbons into helical ribbons. *J. Am. Chem. Soc.* **2010**, *132*, 8819−8821.
(51) Wu, J. C.; Chen, C. C.; Chen, K. H.; Chang, Y. C. Controlled growth of aligned α -helical-polypeptide brushes for tunable electrical conductivity. *Appl. Phys. Lett.* **2011**, *98*, 133304.
(52) Zhao, P.; Liu, D. S.; Wang, P. J.; Zhang, Z.; Fang, C. F.; Ji, G. M. First-principles study of the electronic transport properties of the anthraquinone-based molecular switch. *Phys. B* **2011**, *406*, 895−898.
(53) Song, Z.; Xu, T.; Gordin, M. L.; Jiang, Y.; Bae, I.; Xiao, Q.; Zhan, H.; Liu, J.; Wang, D. Polymer−graphene nanocomposites as ultrafast-charge and-discharge cathodes for rechargeable lithium batteries. *Nano Lett.* **2012**, *12*, 2205−2211.
(54) Yang, M.; Kotov, N. A. Nanoscale helices from inorganic materials. *J. Mater. Chem.* **2011**, *21*, 6775−6792.
(55) Palmer, L. C.; Stupp, S. I. Molecular self-assembly into one-dimensional nanostructures. *Acc. Chem. Res.* **2008**, *41*, 1674−1684.
(56) Bedi, R. K.; Bhatia, S.; Kaur, N.; Kumar, S. Structural and electrical properties of 1, 8bis(3-hydroxypropylamino) and 1-(3-hydroxypropylamino)-9,10-anthraquinone films. *Jpn. J. Appl. Phys.* **2008**, *47*, 8973−8977.
(57) Lee, C. J.; Kang, J. S.; Park, Y. T.; Rezaul, K. M.; Lee, M. S. Study of substitution effect of anthraquinone by SERS spectroscopy. *Bull. Korean Chem. Soc.* **2004**, *25*, 1779−1783.
(58) Rao, B. V.; Choudhary, V.; Varma, I. K. Synthesis and properties of some anthraquinone dyes. *J. Soc. Dyers Colour.* **1990**, *106*, 388−394.
(59) Yeagle, P. L. In *The Structure of Biological Membranes*, 2nd ed.; CRC Press: Boca Raton, FL, 2005; Chapter 5, pp 173−183.

DOI: 10.1021/acs.langmuir.6b00350
Langmuir 2016, 32, 5324−5332